Vegetation Type and Decomposition Priming Mediate Brackish Marsh Carbon Accumulation Under Interacting Facets of Global Change

Anthony J. Rietl[1†], J. Patrick Megonigal[2], Ellen R. Herbert[1††], Matthew L. Kirwan[1]

[1] Virginia Institute of Marine Science, William and Mary, Gloucester Point, VA

[2] Smithsonian Environmental Research Center, Edgewater, MD

Corresponding author: Anthony Rietl (Anthony.Rietl@Wildlife.CA.gov)

Current affiliations:

[†]California Department of Fish and Wildlife, West Sacramento, CA

[††] Ducks Unlimited, Memphis, TN

Key Points:

- Soil priming and species-specific vegetation responses reduce the impacts of elevated CO_2 on marsh sustainability and carbon accumulation
- The relationship between sea level rise and carbon accumulation is driven by changes in soil volume rather than carbon concentration
- The primary impact of elevated CO_2 on carbon accumulation is to extend the lifespan of a marsh under accelerated sea level rise.

Abstract

Coastal wetland carbon pools are globally important, but their response to interacting facets of global change remain unclear. Numerical models neglect species-specific vegetation responses to sea level rise (SLR) and elevated CO_2 (eCO_2) that are observed in field experiments, while field experiments cannot address the long-term feedbacks between flooding and soil growth that models show are important. Here, we present a novel numerical model of marsh carbon accumulation parameterized with empirical observations from a long-running eCO_2 experiment in an organic rich, brackish marsh. Model results indicate that eCO_2 and SLR interact synergistically to increase soil carbon burial, driven by shifts in plant community composition and soil volume expansion. However, newly parameterized interactions between plant biomass and decomposition (i.e. soil priming) reduce the impact of eCO_2 on marsh survival, and by inference, the impact of eCO_2 on soil carbon accumulation.

Plain Language Summary

Coastal marshes are important globally because they tend to capture carbon from the atmosphere in their soils through the activities of plants, which could help moderate the effects of climate change. We developed a numerical computer model based on measurements from a long running elevated carbon dioxide experiment to predict how marshes will change in the future under differing global change scenarios, and how these changes will impact carbon in the soil. We found that elevated carbon dioxide allows marshes to survive faster rates of sea level rise, which in turn allows them to sequester carbon at faster rates. However, we also found that changes in plant communities and their effect on the decomposition of old plant material tends to reduce the overall impacts of elevated carbon dioxide on marsh survival and carbon capture.

1 Introduction

Coastal marshes and their carbon pools adapt to sea level rise largely through ecogeomorphic feedbacks in which increased flooding stimulates plant growth, mineral sediment deposition, and vertical soil development (D'Alpaos et al., 2007; Kirwan and Megonigal, 2013; Marani et al., 2007; Morris et al., 2002). Because plant productivity and organic matter accumulation are inherently linked in anaerobic soils, these ecogeomorphic feedbacks also determine the amount of carbon that marsh soils accumulate through time (Gonneea et al., 2019; Kirwan & Mudd, 2012). Recent work indicates that coastal wetlands are an important global carbon sink (Chmura, 2013; Hopkinson et al., 2012; Mcleod et

al., 2011), and that carbon accumulation rates increase with accelerated sea level rise (Rogers et al., 2019; Wang et al., 2019). Coastal wetlands therefore potentially represent a unique negative carbon-climate feedback where carbon emissions lead to faster rates of sea level rise and enhanced carbon sequestration, making them an important tool towards mitigating changes in the Earth's climate (Crooks et al., 2011; Holmquist et al., 2018).

Nevertheless, the areal extent of coastal marshes has declined worldwide (Duarte, 2008), and there are concerns over the stability of coastal carbon pools in the face of interacting components of global change. Previous numerical modeling and stratigraphic observations suggest that the elevation of marshes and the size of their carbon pools increase with sea level rise until some threshold rate, beyond which they drown (Kirwan et al., 2010; Morris et al., 2002). Elevated CO_2 (eCO_2) increases marsh elevation gain in both short-term field experiments (Langley et al., 2009; Reef et al., 2017) and long-term modeling efforts (Ratliff et al., 2015), but how the interacting effects of SLR and eCO_2 influence marsh resilience and carbon accumulation over decades to centuries is poorly understood. Empirical studies suggest that eCO_2 increases soil carbon in terrestrial systems up to a saturation point (Heimann & Reichstein, 2008; van Groenigen et al., 2014) and may make coastal marshes more resilient to SLR by increasing soil elevation via C_3 plant productivity (Langley et al., 2009; Reef et al., 2017). However, increases in plant productivity may in turn lead to increased decay of older carbon via root-derived inputs of organic carbon and delivery of oxygen into an otherwise anaerobic soil, thereby decreasing the belowground carbon pool (Bernal et al., 2017; Jones et al., 2018; Mueller et al., 2015; Wolf et al., 2007). Vegetation growth leads to a persistent oxygenated zone in wetland sediments (Marani et al., 2006; Boaga et al., 2014), and root induced priming has been shown to be a key factor in regulating the direction of change in terrestrial carbon stocks (Groenigen et al., 2014). However, the importance of priming relative to other drivers remains unexplored in coastal carbon pools.

Vegetation type may also be a strong driver of marsh carbon accumulation under SLR and eCO_2. Due to the relatively stressful conditions in coastal marshes, many plant species have evolved to use the C_4 photosynthetic pathway, which unlike C_3 plants, utilizes a CO_2 concentrating mechanism that negates CO_2 limitation. Thus, as opposed to studies of the effects of eCO_2 on elevation in C_3 marshes, C_4 vegetation has been shown to exhibit little to no response to eCO_2 (Bernal et al., 2017; Morris & Bowden, 1986; Mueller et al., 2015). Previous modeling neglects these differences in vegetation community response for simplicity and because of inherent difficulties separating the effects of eCO_2 in mixed C_3/C_4 communities (Ratliff et al., 2015). Thus, a gap remains between short-term field

experiments that show the importance of vegetation type, and long-term model experiments that suggest the importance of elevation dependent feedbacks. Here, we demonstrate with a novel soil-cohort model that eCO$_2$ and SLR interact synergistically to increase soil carbon burial, driven by shifts in plant community composition, that facilitate an ever-expanding soil volume.

2 Model Description

Our model is designed to simulate changes in the elevation and carbon content of a soil column at a single point on a marsh surface through time, and in response to environmental drivers such as SLR and eCO$_2$. Following previous soil-cohort approaches (Kirwan & Mudd, 2012; Morris & Bowden, 1986), soil cohorts are built annually through the deposition of mineral and organic sediment on the marsh surface and each cohort expands and contracts through time according to organic matter production and decomposition within the soil column. As in previous approaches, mineral deposition and organic matter production vary with the depth and duration of tidal inundation of the marsh surface, and organic matter production and decomposition decrease exponentially with depth below the soil surface. These models demonstrate that marsh elevations and carbon stocks equilibrate to moderate rates of SLR, whereby rates of soil formation equal rates of SLR, but drown under higher rates of SLR (Kirwan & Mudd, 2012; Mudd et al., 2009).

Previous modeling efforts have focused on capturing only the most essential ecomorphodynamic interactions, neglecting many plant and microbial feedbacks that determine carbon preservation (Spivak et al., 2019). Here, we extend their utility by expanding the treatment of vegetation growth, belowground production, and decomposition to include nuanced feedbacks between vegetation type, eCO$_2$, and organic matter priming. We consider two vegetation communities, a C_4 marsh parameterized for *Spartina patens* and a C_3 marsh parameterized for *Schoenopletus americanus,* both common tidal marsh species across North America. At elevations where species overlap, our model creates mixed communities with productivity and decomposition parameterizations weighted according to the relative species distribution. Organic matter decomposition rates increase as aboveground biomass increases (Jones et al., 2018; Mueller et al., 2015), reflecting priming of soil organic matter decomposition associated with root exudation and turnover. The model is used to explore the response of marsh soil carbon to interactions between SLR and eCO$_2$ using observations from the Smithsonian Global Change Research Wetland (GCReW), an organic rich microtidal marsh on a tributary of the Chesapeake Bay (USA) that includes the longest running eCO$_2$ experiment in the world (Drake, 2014).

We parameterized our model using empirical data and a model hindcast to represent conditions similar to a high marsh at GCReW. The entire GCReW site receives negligible mineral sediment, allowing us to simplify lateral gradients in sediment supply, and isolate the effects of dynamic organic matter cycling as drivers of marsh accretion and carbon accumulation. While other modeling experiments on the effects of eCO_2 treated C_3 and C_4 species identically (Ratliff et al., 2015), long-term data at GCReW conclusively shows that eCO_2 increases C_3 biomass production with little effect on C_4 biomass (Langley et al., 2009; Wolf et al., 2007). Our model therefore separates vegetation parameterizations for these fundamental plant functional types and additionally accounts for GCReW data that shows the CO_2 fertilization effect on plant biomass is maximized at an intermediate inundation depth (Langley et al., 2013). Other empirical data used from the site includes tidal range, rooting depth profiles (Megonigal, 1999), species-specific relationships between aboveground biomass and elevation (Byrd et al., 2017), their responses to eCO_2 (Drake, 2014; Groenigen et al., 2014; Langley et al., 2009), and the relationship between decomposition rate and aboveground biomass (Jones et al., 2018; Mueller et al., 2015; Supplementary Table 1).

In order to estimate the parameters for which we did not have data, chiefly the decomposition and turnover rates of belowground biomass, we performed a model hindcast and adjusted unknown parameters until the model produced stratigraphic characteristics consistent with GCReW. This consisted of a spinup period that created an organic rich soil profile in equilibrium with the local late-Holocene rate of relative SLR (~1 mm yr^{-1}), and then a 150-year model run under the historic local rate of SLR (3.6 mm yr^{-1}) observed in Annapolis, MD (NOAA, 2019). The model produced a final marsh elevation (0.34 m NAVD), accretion rate (~3.4 mm yr^{-1}), and soil organic matter profile that are within the range of high marsh characteristics observed at GCReW today (Messerschmidt & Kirwan, 2020; Fig. 1). Also consistent with field observations at GCReW is the modeled loss of elevation relative to sea level (i.e. disequilibrium) (Fig. 1), as evidenced by the increase in flood tolerant C_3 low marsh species encroaching into C_4 high marsh habitat over the past three decades (Lu, *in press*). Taken together, these observations suggest that the model is generally capable of simulating soil-building processes at GCReW and other organic rich marshes.

5 Results & Conclusions

To understand basic model behavior in a submerging marsh, we began our model experiments by subjecting a high elevation C_4 marsh to a rate of SLR high enough to induce rapid drowning (25 mm yr^{-1}; Fig. 2). In these model runs, simulations begin with a marsh elevation (0.43 m NAVD) and organic

rich soil profile created during the model spin-up period under a 1 mm yr^{-1} rate of SLR. Under ambient CO_2 (aCO_2), progressive inundation drives the conversion of a C_4 marsh to a mixed community dominated by C_4 vegetation (> 50%), then to a mixed community dominated by C_3 vegetation, and finally to a C_3 marsh that submerges (Fig. 2a). Accretion for the first 10 years is driven purely by organic inputs into a saturated high marsh that receives no tidal inundation. Although mineral accretion rates then increase through time, driven by longer and deeper flooding of the marsh surface, our parameterization (suspended sediment concentration= 5 mg L^{-1}; tidal amplitude = 0.22 m) limits mineral sediment deposition and ensures that organic matter accumulation dominates marsh elevation change. Under the modeled instantaneous increase in sea level rise rate (1 to 25 mm yr^{-1}), organic accretion rates initially increase from ~ 1 mm yr^{-1} to 4 mm yr^{-1} (Fig. 2a) as production of C_4 vegetation exceeds decomposition (Fig. 2b). As vegetation shifts to more flood tolerant C_3 vegetation with slower parameterized root turnover, organic accretion rates decline, and the marsh eventually drowns (Fig. 2a). Total carbon summed over the entire profile increases throughout the experiment, even as instantaneous carbon accumulation rates fluctuate during conversion to C_3 vegetation (Fig. 2b).

Under eCO_2 conditions, the model predicts qualitatively similar results (i.e. identical accretion rates for the C_4 vegetation community, fluctuation in organic matter accumulation driven by vegetation type, and eventual submergence of the marsh platform). However, the positive effect of eCO_2 on C_3 vegetation growth allows the marsh to survive longer than under aCO_2 (Fig. 2c). Elevated CO_2 prolonged a state change from tidal marsh to open water by over a decade under the accelerated rate of SLR applied in this modeling exercise (25 mm yr^{-1}), a response that would likely translate into several decades under most contemporary SLR scenarios. This behavior is driven by a bigger difference between enhanced production and decomposition than under aCO_2 (Fig. 2d), and a more persistent mixed community where rapid C_4 turnover accompanies C_3 growth enhanced by eCO_2, resulting in a synergistic enhancement of organic matter accumulation (Fig. 2c). Total organic matter and carbon summed across the soil profile are higher under eCO_2 (Fig. 2d) than aCO_2 (Fig. 2b), indicating that the priming effect of plant biomass under eCO_2 does not completely offset the increase in organic production.

Next, we conducted three separate model runs at 25 mm yr^{-1} to explore how our novel parameterizations influence model behavior relative to approaches used in previous models, and in particular, the approaches used in the only other eCO_2-informed tidal marsh model (Ratliff et al., 2015). Our model differs from previous models in two key ways: 1) we parameterize C_3 and C_4 species

separately to include a CO_2 fertilization effect on C_3 species only, as opposed to the assumption that *e*CO_2 affects all vegetation (Ratliff et al., 2015), and 2) our model incorporates a previously unexplored priming effect where decomposition fluctuates with plant productivity due to the introduction of fresh carbon, and/or radial oxygen loss from roots and rhizomes (Jones et al., 2018; Mueller et al., 2015). This means our decay rate is dynamic, changing throughout a model simulation as opposed to a static value. In these experiments, both species-specific *e*CO_2 responses and organic matter priming lead to faster marsh drowning relative to the constraints of previous model (Fig. 3). However, we also find that priming has a much stronger effect than the species-specific *e*CO_2 parameterization (Fig. 3). This surprising behavior is illustrated by the substantial difference in biomass produced between runs with and without species-specific effects, and yet little difference in the time until marsh submergence. These strikingly similar results occur because the increase in biomass of the C_4 community under *e*CO_2 is counterbalanced by an increase in decomposition in our model (Fig. 3). This highlights an important aspect of our model, that production and decomposition are tightly coupled through time due to the plant-mediated priming effect and suggests that previous model results may overestimate the positive effects of *e*CO_2 on marsh resilience (Ratliff et al., 2015).

To understand the interactive effect of *e*CO_2 and SLR on marsh resilience and carbon accumulation rate, we subjected a high elevation C_4 marsh to progressively faster rates of SLR and ran the model until it either equilibrated to the new rate of SLR or drowned. These simple model experiments illustrate that carbon accumulation rates (Fig. 4) and total carbon in the soil profile (Fig. 5) increase with increasing rates of SLR until the point of marsh drowning. Interestingly, increases in soil carbon occur even as soils became more mineral rich, driven by surficial sediment deposition that increased with tidal inundation (Fig. 5). Although this model behavior is consistent with faster burial and more efficient carbon preservation, we suggest it is more likely due to mineral deposition rates that increase more quickly than organic matter production rates, resulting in a *relative* decrease in percent organic matter (i.e. a decrease in carbon concentration). In contrast to terrestrial systems in which carbon accumulation is driven by changes in carbon concentration (Lu et al., 2019; Stewart et al., 2007), our results uniquely illustrate that marsh carbon pools are driven by changes in soil volume.

Our finding that carbon accumulation rates increase with the rate of SLR is consistent with previous modeling and stratigraphic observations that attribute accelerating rates of carbon accumulation to the reduction in carbon-sequestration saturation effects associated with an ever-expanding soil volume (Rogers et al., 2019). However, the explicit modeling of the interaction between *e*CO_2 and SLR leads to

new insights into the mechanisms responsible for increasing carbon accumulation. For example, based on inundation alone, organic matter production decreases as marshes transition from pure C_4 to mixed communities (Fig. 2a), but under eCO$_2$ C_3 productivity more than compensates for the decline in productivity, and carbon accumulation rates increase (Fig. 2d). This finding is qualitatively similar to previous modeling demonstrating that SLR and temperature warming lead to an increase in carbon accumulation rates (Kirwan & Mudd, 2012), but in those model experiments warming did not enhance marsh persistence. Here, our results show that eCO$_2$ extends marsh persistence where SLR drives the conversion of C_4 vegetation to C_3 vegetation that accumulates organic matter faster under eCO$_2$ (Fig. 4). In these experiments, marshes drown when SLR rates exceed 4 and 11 mm yr^{-1} under aCO$_2$ and eCO$_2$ respectively. Although specific threshold rates of SLR and the quantitative effect of eCO$_2$ on marsh accretion depend on model parameterizations, increased marsh resilience is generally consistent with empirical field experiments (Langley et al., 2009; Reef et al., 2017). Thus, the primary influence of eCO$_2$ is to allow the marsh to survive faster rates of SLR, which in turn facilitates soil volume expansion, and faster carbon accumulation (Fig. 4).

Acknowledgments, Samples, and Data

This material is based upon work supported by the US Department of Energy, Office of Science, Office of Biological and Environmental Research Program (DE-SC0014413 and DE-SC0019110), the National Science Foundation CAREER Program (EAR-1654374), and the Smithsonian Institution. We have uploaded organic content, accretion rate, and root distribution data used to paramterize and test the numerical model. The organic content and accretion rate data is available at https://doi.org/10.25573/serc.11914140.v1. The root distribution data is available at https://doi.org/10.25573/serc.13073249. All other data used to parameterize or test the numerical model is already published or otherwise publically available.

References

Agren, G.I., & Ingestad, T. (1987). Root:shoot ratio as a balance between nitrogen productivity and photosynthesis. *Plant, Cell & Environment*, 10, 579-586

Bernal, B., Megonigal, J.P. & Mozdzer, T.J. (2017). An Invasive wetland grass primes deep soil carbon pools. *Global Change Biology,* 23, 2104-2116

235 Boaga, J., D'Alpaos, A., Cassiani, G., Marani, M., & Putti, M. (2014). Plant-soil interactions in salt
236 marsh environments: Experimental evidence from electrical resistivity tomography in the Venice
237 Lagoon. *Geophysical Research Letters,* 41, 6160– 6166. https://doi.org/10.1002/2014GL060983
238 Bradley, P.M., & Morris, J.T. (1990). Influence of oxygen and sulfide concentration on nitrogen uptake
239 kinetics in Spartina alterniflora. *Ecology,* 71, 282-287
240 Byrd, K.B., Ballanti, L.R., Thomas, N.M., Nguyen, D.K., Holmquist, J.R., Simard, M., et al. (2017).
241 Tidal marsh biomass field plot and remote sensing datasets for six regions in the conterminous
242 United States (ver. 2.0, June, 2020): U.S. Geological Survey data release.
243 Chmura, G.L. (2013). What do we need to assess the sustainability of the tidal saltmarsh carbon sink?
244 *Ocean and Coastal Management,* 83, 25-31
245 Craft, C.B., Seneca, E.D., & Broome, S.W. (1991). Loss on ignition and Kjeldahl digestion for
246 estimating organic carbon and total nitrogen in estuarine marsh soils: calibration with dry
247 combustion. *Estuaries,* 14, 175-179
248 Crooks, S., Herr, D., Tamelander, J., Laffoley, D. & Vandever, J. (2011). Mitigating climate change
249 through restoration and management of coastal wetlands and near-shore marine ecosystems:
250 challenges and opportunities. *Environment Department Paper,* 121**,** World Bank, Washington,
251 DC.
252 Curtis, P.S., Balduman, L.M., Drake, B.G. & Whigham, D.F. (1990). Elevated atmospheric CO_2 effects
253 on belowground processes in C_3 and C_4 estuarine marsh communities. *Ecology,* 71, 2001-2006
254 D'Alpaos, A., Lanzoni, S., Marani, M., & A. Rinaldo. (2007). Landscape evolution in tidal embayments:
255 modeling the interplay of erosion, sedimentation, and vegetation dynamics. *Journal of*
256 *Geophysical Research,* 112, F1. https://doi.org/10.1029/2006JF000537
257 Drake, B.G. (2014). Rising sea level, temperature, and precipitation impact plant and ecosystem
258 responses to elevated CO_2 on a Chesapeake Bay wetland: review of a 28-year study. *Global*
259 *Change Biology,* 20, 3329-3343
260 Duarte, C.M., Dennison, W.C., Orth, R.J.W. & Carruthers, T.J.B. (2008). The charisma of coastal
261 ecosystems: addressing the imbalance. *Estuaries and Coasts,* 31, 233-238
262 Gill, R.A. & Jackson, R. (2000). Global patterns of root turnover for terrestrial ecosystems. *New*
263 *Phytologist,* 147, 13-31

264 Giurgevich, J.R., & Dunn, E.L. (1981). A comparative analysis of the CO2 and water vapor response of
265 two Spartina species from Georgia coastal marshes. *Estuarine, Coastal, and Shelf Science,* 12,
266 561-568
267 Gonneea, M.E., Maio, C.V., Kroeger, K.D., Hawkes, A.D., Mora, J., Sullivan, R., et al. (2019). Salt
268 marsh ecosystem restructuring enhances elevation resilience and carbon storage during
269 accelerating relative sea-level rise. *Estuarine, Coastal, and Shelf Science,* 217, 56-68
270 Gulde, S., Chung, H., Amelung, W., Chang, C., & Six, J. (2008). Soil carbon saturation controls labile
271 and stable carbon pool dynamics. *Soil Science Society of America Journal,* 72, 605-612
272 Heimann, M. & Reichstein, M. (2008). Terrestrial ecosystem carbon dynamics and climate feedbacks.
273 *Nature,* 451, 289-292
274 Holmquist, J.R., Windham-Myers, L., Bliee, N., Crooks, S., Morris, J.T., Megonigal, J.P., et al. (2018).
275 Accuracy and precision of tidal wetland soil carbon mapping in the conterminous United States.
276 *Scientific Reports*, 8, 9478
277 Hopkinson, C.S., Morris, J.T., Fagherazzi, S., Wollheim, W.M. & Raymond, P.A. (2018).Lateral marsh
278 edge erosion as a source of sediments for vertical marsh accretion. *JGR Biosciences,* 123, 2444-
279 2465. https://doi.org/10.1029/2017JG004358
280 Hopkinson, C.C., Wei-Jun, C. & Hu, X. (2012). Carbon Sequestration in wetland dominated coastal
281 systems - a global sink of rapidly diminishing magnitude. *Current Opinion in Environmental*
282 *Sustainability,* 4, 186-194
283 Jan van Groenigen, K., Qi, X., Osenberg, C.W., Luo, Y. & Hungate, B.A. (2014). Faster decomposition
284 under increased atmospheric CO_2 limits soil carbon storage. *Science*, 344, 508-509
285 Jones, S.F., Stagg, C.L., Krauss, K.W. & Hester, M.W. (2018). Flooding alters plant-mediated carbon
286 cycling independently of elevated atmospheric CO_2 concentrations. *Journal of Geophysical*
287 *Research: Biogeosciences,* 123, 1976-1987. https://doi.org/10.1029/2017JG004369
288 Kirwan, M.L. & Gutenspergen, G.R. (2015). Response of plant productivity to experimental flooding in
289 a stable and a submerging marsh. *Ecosystems,* 18, 903-913
290 Kirwan, M.L., Guntenspergen, G.R., D'Alpaos, A., Morris, J.T., Mudd, S.M. & Temmerman, S. (2010).
291 Limits on the adaptability of coastal marshes to rising sea level. *Geophysical Research Letters,*
292 37, L23401. https://doi.org/10.1029/2010GL045489
293 Kirwan, M.L. & Mudd, S.M. (2012). Response of sat-marsh carbon accumulation to climate change.
294 *Nature,* 489, 550-553

Kirwan, M.L. & Megonigal, J.P. (2013). Tidal wetland stability in the face of human impacts and sea-level rise. *Nature,* 504, 53-60

Langley, J.A., McKee, K.L., Cahoon, D.R., Cherry, J.A. & Megonigal, J.P. (2009). Elevated CO_2 stimulates marsh elevation gain, counterbalancing sea-level rise. *Proceedings of National Academy of Sciences, 106,* 6182-6186

Langley, J.A., Mozdzer, T.J., Shepard, K.A., Hagerty, S.B., Megonigal, J.P. (2013). Tidal marsh plant responses to elevated CO_2, nitrogen fertilization, and sea level rise. *Global Change Biology,* 19, 1495-1503

Lu, M., Herbert, E.R., Langley, J.A., Kirwan, M.L., Megonigal, J.P. (2019). Nitrogen status regulates morphological adaptation of marsh plants to elevated CO_2. *Nature Climate Change, 9, 764-768*

Marani, M., Silvestri, S., Belluco, E., Ursino, N., Comerlati, A., Tosatto, O.,et al. (2006). Spatial organization and ecohydrological interactions in oxygen-limited vegetation ecosystems. *Water Resources Research,* 42, W06D06

Marani, M., D'Alpaos, A., Lanzoni, S., Carniello, L. & Rinaldo, A. (2007). Biologically controlled multiple equilibria of tidal landforms and the fate of the Venice lagoon. *Geophysical Research Letters,* 34, L11402. https://doi.org/10.1029/2007GL030178

Marani, M., D'Alpaos, A., Lanzoni, S., Carniello, L., & Rinaldo, A. (2010). The importance of being coupled: stable states and catastrophic shifts in tidal biomorphodynamics. *Journal of Geophysical Research,* 115, F4. https://doi.org/10.1029/2009JF001600

Mcleod, E., Chmura, G.L., Bouillon, S., Salm, R., Bjork, M., Duarte, C.M., et al. (2011). A blueprint for blue carbon: toward an improved understanding of the role of vegetated coastal habitats in sequestering CO_2. *Frontiers in Ecology and the Environment,* 9, 552-560

Megonigal, J.P. et al. 1999 (2020) CO_2 x community deep root biomass. Dataset DOI: 10.25573/serc.13073249, https://figshare.com/s/6829ad2d6a501d6538fe

Messerschmidt, T.C. & Kirwan, M.L. (2020). Dataset: Soil properties and accretion rates of C_3 and C_4 marshes at the Global Change Research Wetland, Edgewater, Maryland. figshare. Dataset. https://doi.org/10.25573/serc.11914140.v1

Morris, J.T., Barber, D.C., Callaway, J.C., Chambers, R., Hagen, S.C., Hopkinson, C.S., Johnson, B.J., Megonigal, P., Neubauer, S.C., Troxler, T., & Wigand, C. (2016). Contributions of organic and inorganic matter to sediment volumes accretion in tidal wetlands at steady state. *Earth's Future,* 4, 110-121

Morris, J.T. & Bowden, W.B. (1986). A mechanistic, numerical model of sedimentation, mineralization, and decomposition for marsh sediments. *Soil Science Society of America Journal,* 50, 96-105

Morris, J.T., Sundareshwar, P.V., Nietch, C.T., Kjerfve, B. & Cahoon, D.R. (2002). Responses of coastal wetland to rising sea level. *Ecology, 83,* 2869-2877

Mudd, S.M., Howell, S.M. & Morris, J.T. (2009). Impact of dynamic feedbacks between sedimentation, sea-level rise, and biomass production on near-surface marsh stratigraphy and carbon accumulation. *Estuarine, Coastal and Shelf Science,* 82, 377-389

Mueller, P., Jensen, K. & Megonigal, J.P. (2015). Plants mediate soil organic matter decomposition in response to seal level rise. *Global Change Biology,* 22, 404-414

NOAA. (2019). Relative Sea Level Trend for Station 8575512, Annapolis Maryland. https://tidesandcurrents.noaa.gov/sltrends/sltrends_station.shtml?id=8575512

Ratliff, K.M., Braswell, A.E. & Marani, M. (2015). Spatial response of coastal marshes to increased atmospheric CO_2. *Proceedings of National Academy of Sciences,* 112, 15580-15584

Reef, R., Spencer, T., Moller, I., Lovelock, C.E., Christie, E.K., Mcivor, A.L., et al. (2017). The effects of elevated CO_2 and eutrophication on surface elevation gain in a European salt marsh. *Global Change Biology,* 23, 881-890

Reynolds, H.L., & D'Antonio, C. (1996). The ecological significance of plasticity in root weight in response to nitrogen. *Plant and Soil*, 185, 75-97

Reynolds, J.F., & Thornley, J.H.M. (1982). A shoot:root partitioning model. *Annals of Botany,* 49, 585-597

Rogers, K., Kelleway, J.J., Saintilan, N., Megonigal, J.P., Adams, J.B., Holmquist, J.R., et al. (2019). Wetland carbon storage controlled by millennial-scale variation in relative sea-level rise. *Nature,* 567, 91-95

Spivak, A.C., Sanderman, J., Bowen, J.L., Canuel, E.A. & Hopkinson, C.S. (2019). Global-change controls on soil-carbon accumulation and loss in coastal vegetated ecosystems. *Nature Geoscience,* 12**,** 685-692

Stewart, C.E., Paustian, K., Conant, R.T., Plante, A.F., Six, J. (2007). Soil carbon saturation: concept, evidence and evaluation. *Biogeochemistry,* 86, 19-31

Van de Broek, M., Vandendriessche, C., Poppelmonde, D., Merckx, R., Temmerman, S. & Govers, G. (2018). Long-term organic carbon sequestration in tidal marsh sediments is dominated by old-aged allochthonous inputs in a macrotidal estuary. *Global Change Biology,* 24, 2498-2512

Wang, F., Xiaoliang, L., Sanders, J.C. & Tang, J. (2019). Tidal wetland resilience to sea level rise increases their carbon sequestration capacity in United States. *Nature Communications,* 10**,** 5434

Wolf, A.A., Drake, B.G., Erickson, J.E. & Megonigal, J.P. (2007). An oxygen-mediated positive feedback between elevated carbon dioxide and soil organic matter decomposition in a simulated anaerobic wetland. *Global Change Biology,* 13, 2036-2044

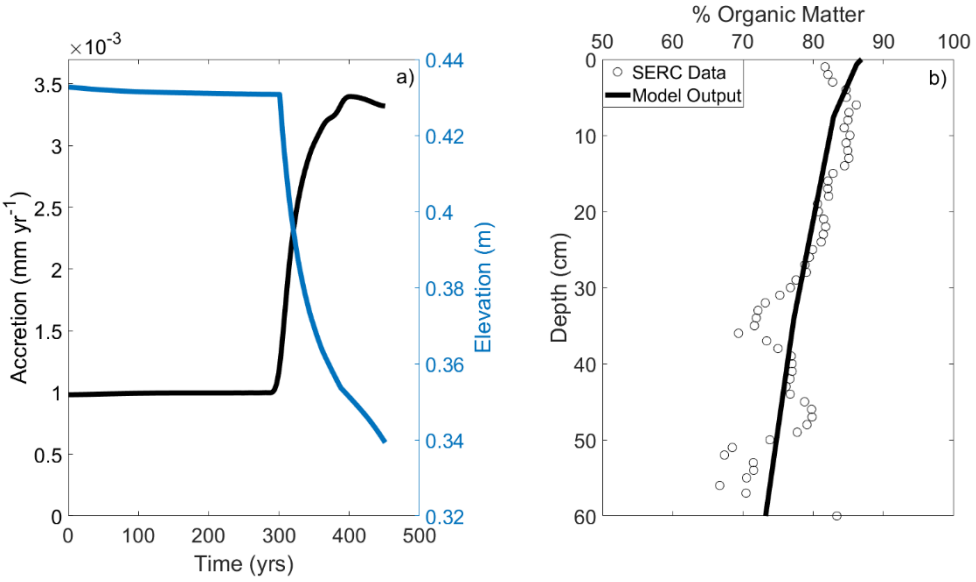

Figure 1. A hindcast model validation experiment in which an organic marsh equilibrated to a historic sea level rise rate of 1 mm yr^{-1} was subjected to a modern rate of sea level rise at Kirkpatrick Marsh (3.6 mm yr^{-1}) for 150 years to recreate current conditions. a) Accretion rate (mm yr^{-1}; black line) and Elevation relative to sea level (m; blue line), b) Percent organic matter (LOI) for model output (black line) and field data from Kirkpatrick Marsh (open circles).

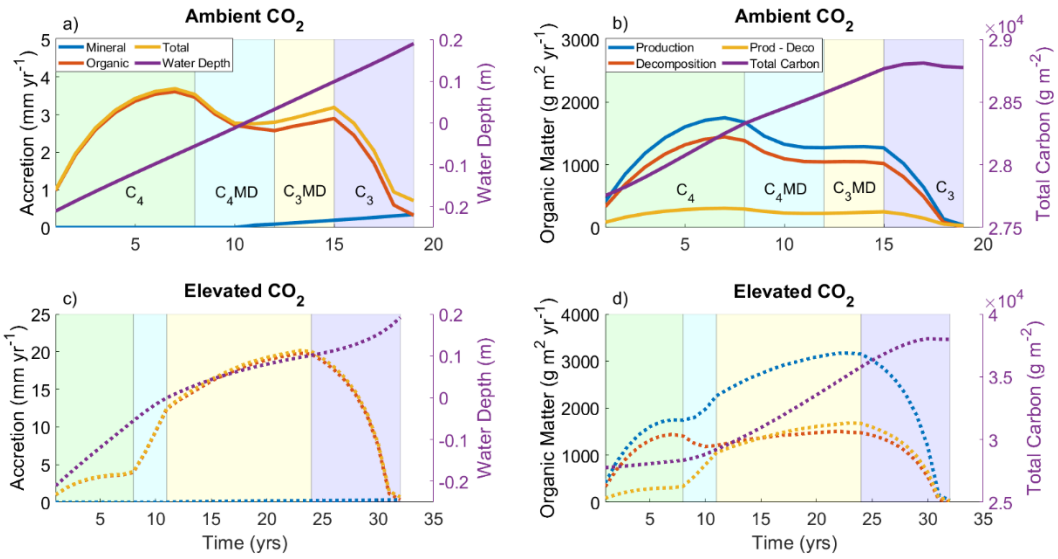

Figure 2. Results from a model experiment in which an organic marsh equilibrated to a sea level rise rate of 1 mm yr^{-1} was subjected to a sea level rise rate of 25 mm yr^{-1} in order to induce submergence under ambient and elevated CO_2 conditions. Background panel colors represent vegetation types; a C_4 (green), C_4 dominant (>50%) mixed (C_4MD; blue), C_3 dominant (>50%) mixed (C_3MD; yellow), and C_3 (purple) community. a) Accretion rate (organic, mineral, and total) and water depth above marsh surface at mean high tide for a submerging marsh under ambient CO_2 conditions, b) Organic matter dynamics (production, decomposition, and net accumulation), and total carbon (g m^{-2}) in the marsh soil profile for a submerging marsh under ambient CO_2 conditions, c) Accretion rate and water depth above marsh surface for a submerging marsh under elevated CO_2 conditions, d) Organic matter dynamics and total carbon in the soil profile for a submerging marsh under elevated CO_2 conditions. Note the differring scales of the x-axes, and that negative water depths indicate a supratidal position of the marsh relative to mean high tide.

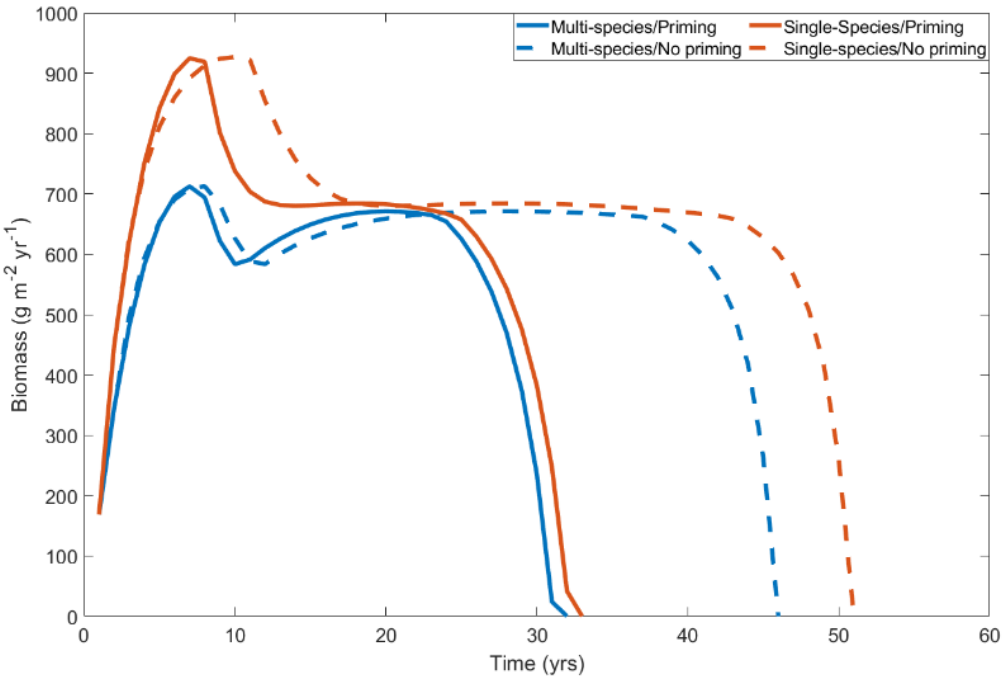

Figure 3: Aboveground biomass production through time for model experiments employing the methodological constraints of Ratliff et al. (2015) (a non-species-specific CO_2 effect and no priming). Multi-species refers to our model parameterization that includes a positive CO_2 effect on C_3 vegetation but not C_4 vegetation and priming refers to our model's incorporated priming effect on decomposition. Each model experiment began by subjecting an organic marsh equilibrated to a sea level rise rate of 1 mm yr^{-1} to a sea level rise rate of 25 mm yr^{-1}.

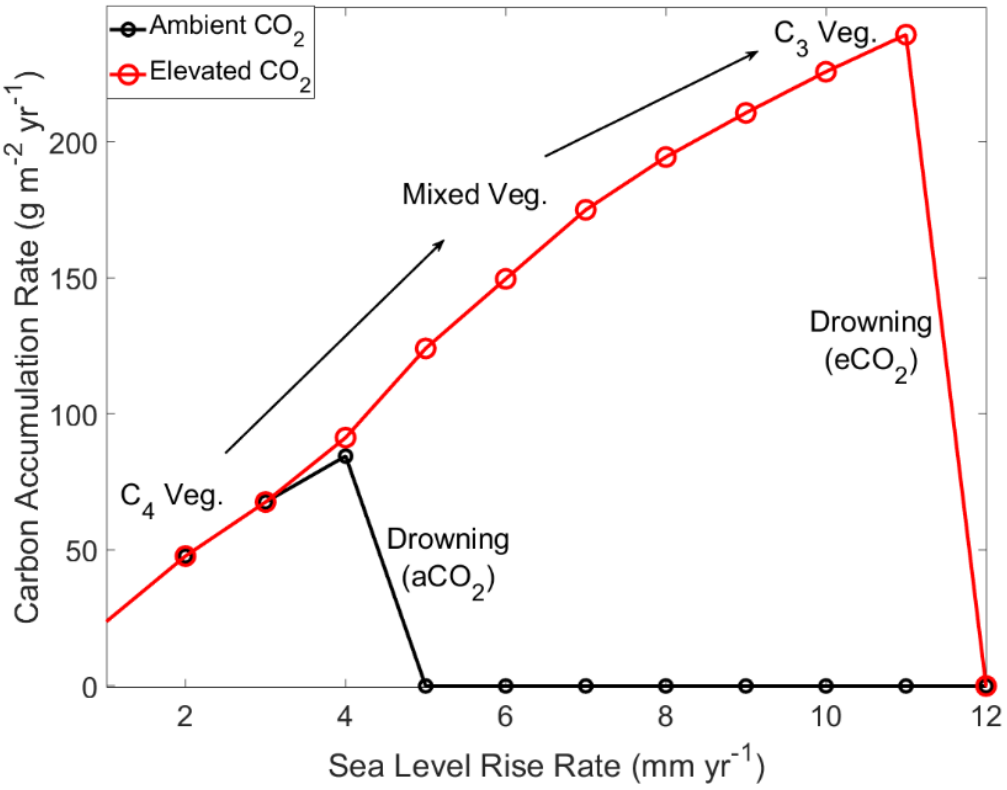

Figure 4: Results from model equilibration experiments in which a high elevation C_4 marsh was subjected to progressively faster rates of sea level rise under ambient and elevated CO_2. Carbon accumulation rates (g m^{-2} yr^{-1}) under ambient (black open circles) and elevated (red open circles) CO_2 at sea level rise rates between 1 and 12 mm yr^{-1}. Marsh drowns when sea level rise exceeds 4 mm yr^{-1} under *a*CO_2 (black line) and 11 mm yr^{-1} under *e*CO_2 (red line). There is no effect of *e*CO_2 on CAR at low sea level rise rates because the marsh equilibrates to elevations too high for C_3 vegetation.

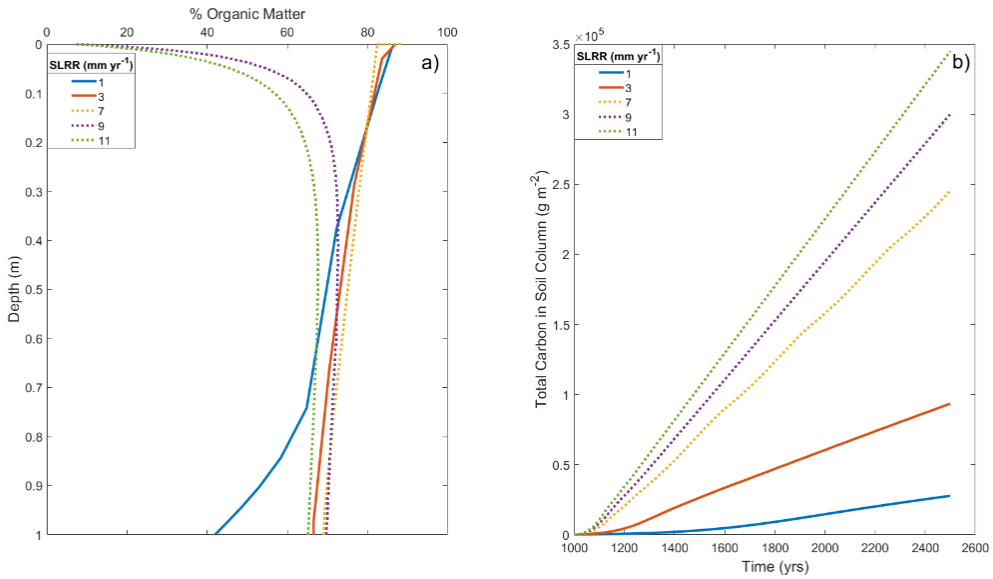

Figure 5: Results from model equilibration experiments in which a high elevation C_4 marsh was subjected to progressively faster rates of sea level rise under ambient and elevated CO_2. a) Percent organic matter (LOI) for progressively faster sea level rise rates under ambient (solid lines) and elevated (dashed lines) CO_2 conditions, b) total carbon (g m^{-2}) in the marsh soil profile for progressively faster sea level rise rates under ambient (solid lines) and elevated (dashed lines) CO_2 conditions.

AGU PUBLICATIONS

[Geophysical Research Letters]

Supporting Information for

Vegetation Type and Soil Priming Drive Marsh Carbon Accumulation Under Interacting Facets of Global Change

Anthony J. Rietl[1†], J. Patrick Megonigal[2], Ellen R. Herbert[1††], Matthew L. Kirwan[1]

[1] Virginia Institute of Marine Science, William and Mary, Gloucester Point, VA

[2] Smithsonian Environmental Research Center, Edgewater, MD

Contents of this file

1 Model Description

Our model is designed to simulate changes in the elevation and carbon content of a soil column at a single point on a marsh surface through time in response to sea level rise and elevated CO_2. Following the approach taken in other marsh soil cohort models (Morris & Bowden, 1986; Mudd et al., 2009), our model considers the evolution of a soil column discretized into cohorts (Q(t)) that represent layers of soil of a given age (t). New cohorts are added annually to the surface of the soil column through the deposition of sediment from semidiurnal tides and advected lower in the soil column as they age, such that the oldest cohort (*Q(1),* deposited at t=1) is at the bottom and the most recently

deposited at the top (Q(t+1). The thickness of each cohort evolves through time as live roots and decaying organic matter are deposited within the soil column. The vertical expansion and contraction of soil cohorts directly translates into changes in marsh elevation. Thus, much like previous models of saltmarsh vertical accretion (D'Alapos et al., 2007; Marani et al., 2007; Morris et al., 2002; Ratliff et al., 2015), marsh elevation change in our model occurs through the cumulative changes in mineral and organic inputs. At each time step, the model determines sediment deposition on the marsh surface, vegetation type (C_3, C_4, or mixed), and organic matter production and decomposition that together describe changes in marsh elevation through time. Here, we describe each of these processes in detail. Dimensions are denoted in square brackets of [M] for mass, [L] for length, and [T] for time.

1.1 Allochthonous Sediment Deposition

Sediment is deposited on the marsh surface as a function of the height and duration of tidal flooding, and the availability of suspended sediment in the water column. Following previous approaches (D'Alapos et al., 2007), the annual mass of sediment deposited (q_s) is calculated as:

$$q_s = \int_T C_t \, w_s \, dt \qquad \textbf{(1)}$$

where q_s [M L^{-2} T^{-1}] is sediment settling as defined by the product of the settling velocity (w_s) [L T^{-1}], and the instantaneous suspended sediment concentration C_t [M L^{-3}] integrated over the tidal cycle dt [T]. Following previous approaches (Marani et al., 2010), C_t is constant on the rising flood tide, but declines throughout the ebbing phase as the difference between the depth integrated mass of sediment coming onto the marsh from tides with a fixed concentration of sediment (C_o) and the cumulative mass of sediment deposited on the marsh surface at time t. In these simulations, we chose C_o = 5 mg/L to represent organic rich marshes far from tidal channels, like those at the Smithsonian Global Change Research Wetland (GCReW). The mass of sediment deposited on the marsh surface depends on the height and duration of tidal inundation, which is calculated over one average tidal cycle and extrapolated to an annual time step by multiplying by the number of tidal cycles in a year. Other numerical models consider the influence of vegetation on sediment deposition, and lateral gradients in sediment supply (D'Alapos et al., 2007; Marani et al., 2010; Ratliff et al., 2015). In contrast, we

intentionally focus our modeling efforts on conditions (low tide range, low C_o) that lead to negligible mineral sediment deposition so that we can isolate the effects of dynamic organic matter cycling on carbon accumulation and elevation change.

1.2 Vegetation

The growth and type of vegetation is also related to tidal inundation. Following previous approaches (Morris et al., 2002; Mudd et al., 2009), the aboveground biomass of vegetation is defined by a parabolic relationship with marsh surface elevation relative to sea level (Supp. Fig. 1), which is a proxy for flooding duration and associated environmental factors. In our model, we use biomass-elevation relationships for two common species at GCReW (Byrd et al., 2017). These species represent plants with different carbon fixation strategies - *Spartina patens* (C_4) found at the higher elevations with little flooding, and *Schenoplectus americanus* (C_3) found at lower elevations where flooding is common. Marsh elevation relative to sea level in each time step is used to determine which vegetation community is present, or if a mixed community exists, as defined by the parabolic relationship between species biomass and elevation (Supp. Fig. 1). Aboveground biomass for each time step is given by:

$$B = \alpha\, z_{sl}{}^2 + \beta\, z_{sl} + \theta \qquad \textbf{(2)}$$

where aboveground biomass (B) [M L^{-2}] is a function of elevation relative to sea level (z_{sl}) and α, β, θ are coefficients describing the relationship between elevation and biomass at GCReW (Suppl. Table 1; Supp. Fig. 1; Byrd et al., 2017). When species growth curves overlap, resulting in mixed communities, the percentage of each species is calculated as $B_i / (B_i + B_j)$. These percentages are used to calculate a weighted average for all species-specific parameters related to productivity and decomposition in mixed communities. Under $e$$CO_2$ conditions, aboveground biomass in the model increases in C_3 species by a factor of ~ 1.3 and does not increase in C_4 species, as has been observed at GCReW (Drake, 2014; Langley et al., 2009).

Belowground biomass is estimated from aboveground biomass, where rhizomes and roots are considered separately. Rhizome biomass (R_h) [M L^{-2}] is proportional to aboveground biomass:

$$R_h = gB \qquad \textbf{(3)}$$

where g = 1 for ambient conditions and g = 2 for eCO$_2$. Root biomass (R_o) [M L^{-2}] is estimated using a balanced growth model that describes a functional equilibrium in which the mass and uptake of carbon by leaf tissue (B) is balanced by the mass and uptake of nutrients (μ) by root tissue (Reynold & D'Antonio, 1996; Reynold & Thornley, 1982; Agren & Ingestad, 1987).

$$R_o = B\frac{\sigma\tau}{\mu} \qquad \textbf{(4)}$$

where τ is carbon uptake net respiration, σ is an optimal tissue C:N ratio, and μ is a nitrogen uptake rate. Although nutrient uptake by root tissues should be dynamic and species specific, there is not enough information on *S. patens* and *S. americanus* belowground processes to treat these properly in the model. Instead, we use Michaelis-Menton kinetics to calculate a temporally constant N uptake rate based largely on measurements for *S. alterniflora* (Bradley & Morris, 1990; Giurgevich & Dunn, 1981). This approach necessarily leads to a constant root:shoot ratio for each vegetation type and CO$_2$ scenario (R:S = 1.10 for C$_4$ vegetation, 1.79 for C$_3$ vegetation, and 2.15 for C$_3$ vegetation under eCO$_2$). Together, root and rhizome biomass calculations produce a total belowground:aboveground biomass ratio of 2.10 for C$_4$ vegetation, 2.79 for C$_3$ vegetation, and 4.15 for C$_3$ vegetation under eCO$_2$. Like estimates of turnover described below, these model parameters are highly uncertain. Nevertheless, the belowground:aboveground biomass ratios used in the model are consistent with species-specific field measurements from the GCReW site and other Chesapeake Bay brackish marshes. For example, measured root:shoot ratios in these marsh types are generally between 2-5, higher in C$_3$ than C$_4$ vegetation, do not change consistently with flooding (Kirwan & Gutenspergen, 2015), and increase with eCO$_2$ in C$_3$ vegetation (Langley et al., 2013). Following (Morris & Bowden, 1986; Mudd et al, 2009), the total biomass of roots and rhizomes is distributed through the soil profile to a maximum rooting depth below the soil surface as:

$$R_o = \frac{R_{oo}}{\gamma}\, e^{\left(\frac{-d_s}{\gamma}\right)}$$

$$R_h = \frac{R_{ho}}{\gamma}\, e^{\left(\frac{-d_s}{\gamma}\right)} \qquad \textbf{(5)}$$

where γ [L] is the depth at which belowground biomass decreases by approximately one-third (Mudd et al, 2009), and d_s is depth below the soil surface. R_o and R_h are calculated

at the surface *(R_{oo}, R_{ho})* and in each cohort following the scheme of Morris & Bowden, (1986). The masses of live roots and rhizomes (R_o, R_h) [M L^{-2}] are then summed to determine the total biomass produced in each cohort and each time step.

1.3 Organic Matter Accumulation

Organic matter accumulation within the soil column depends on root and rhizome turnover, the organic content of allochthonous sediment deposited on the marsh surface, and decomposition of organic matter. Organic accumulation within a soil cohort (q_o) [M L^{-2} T^{-1}] is given as:

$$q_o = (1-a)(R_o T_o + R_h T_h) + j\, q_s - D \qquad \textbf{(6)}$$

where T_o and T_h [T^{-1}] are the annual turnover of root and rhizome biomass respectively. Belowground biomass enters the soil profile and contributes to organic matter fluxes through turnover. We assume that roots turnover more quickly than rhizomes, and that C_4 plants have faster turnover than C_3 plants (Table 1). This assumption follows the general observation that root turnover increases with decreasing diameter class (Gill & Jackson, 2000), and measurements at GCReW that indicate *S. americanus* rhizomes are larger in diameter than *S. patens* rhizomes (Curtis et al., 1990). Nevertheless, belowground turnover is a poorly understood process, and these parameters were necessarily chosen based on model hindcasts rather than direct measurements. The parameter *a* represents a fraction of organic matter that is composed of non-decaying components of plant tissue (e.g. silica) that remain as ash during loss-on-ignition (LOI) analyses. In the model simulations presented here, we assign *a=0.08* based on LOI derived soil organic fractions that almost never exceed 0.92 at GCReW (Messerschmidt & Kirwan, 2020) and in diverse wetlands across the United States (Morris et al., 2016). The coefficient *j* is the organic fraction of suspended sediment so that jq_s [M L^{-2} T^{-1}] represents allochthonous organic matter. For simplicity, we chose an arbitrary low organic fraction of suspended sediment (j = 0.05) so that organic matter accumulation in the model is driven by autocthonous rather than allochthonous processes. Finally, D [M L^{-2} T^{-1}] is the total amount of organic matter decomposition in a soil cohort as described below.

Following previous approaches (Morris & Bowden, 1986; Mudd et al., 2009; Kirwan and Mudd, 2012), organic matter produced through root and rhizome turnover ($[1-a][R_o T_o + R_h T_h]$) is split into fast decaying (labile), and slow decaying (refractory)

pools. The model experiments here follow the parameterization of Mudd et al., (2009), where the labile organic fraction is 0.84 and the refractory component is 0.16. We additionally consider labile (0.1) and refractory (0.9) fractions of allochthonous organic matter deposition (jq_s). This parameterization is based on the observation that allochthonous organic matter is typically old and recalcitrant (Hopkinson et al., 2018; Van de Broek et al., 2018) but is of limited importance in these simulations where parameters are chosen to minimize allochthonous organic sediment deposition.

The decomposition rate of organic matter in each soil cohort (D) follows a linear decay model,

$$D = \frac{dQ_o}{dt} = -kQ_o \qquad \textbf{(7)}$$

where Q_o [M L^{-2}] represents the total amount of organic matter in each soil cohort (i.e. q_o summed through time). Like previous models, labile and refractory pools have different decay coefficients (k_l and k_r) [T^{-1}]. However, we also modify the decay coefficient in each cohort by its depth below the surface, and the amount of aboveground biomass to represent the effects of soil priming via radial oxygen loss from plant roots. As plant biomass increases, aerobic leakage into the rhizosphere leads to an increase in decomposition (Jones et al., 2018; Mueller et al., 2015; Wolf et al., 2007). For each organic matter pool, a reference decay coefficient (k_{ref}) at the surface of the soil profile is modified by biomass and according to the depth of each cohort below the soil surface. k_{ref} represents a depth-averaged decay rate which is observed for a typical aboveground biomass (B_{ref}) [M L^{-2}]. Once k_{ref} and B_{ref} have been assigned, organic matter decay for the labile and organic pools at the top of the soil profile ($k_{l,o}$ and $k_{r,o}$) [M L^{-2} T^{-1}] are given as:

$$k_{l,0} = k_{l\_ref}\, \nu\left(\frac{B}{B_{ref}}\right)$$

$$k_{r,0} = k_{r\_ref}\, \nu\left(\frac{B}{B_{ref}}\right) \qquad \textbf{(8)}$$

where the coefficient $\nu = 0.5129$ (based on estimates from Wolf et al., (2007)) and B is total aboveground biomass in each time step. Decay at the top of the soil profile is calculated for both labile and refractory organic matter pools as given by the k_{ref} values

for each pool. The decay coefficient for labile and refractory pools in each cohort (k_l and k_r) [T^{-1}] are given as:

$$k_l = k_{l,0}\, \varphi e^{(-\omega d_s)}$$

$$k_r = k_{r,0}\, \varphi e^{(-\omega d_s)} \quad \textbf{(9)}$$

where the k_0 is distributed down the soil profile through each soil cohort to a maximum rooting depth, coefficients φ and ω are 1.1186 and 1.8544 respectively (derived from SERC rooting depth data), and d_s [L] is the depth from the surface of a given cohort.

1.4 Elevation

Marsh elevation change is driven by the change in mass and thickness of individual soil cohorts, integrated throughout the soil profile. The total mass of mineral sediment entering each cohort, q_m [M L^{-2} T^{-1}], depends on sediment deposition during tidal inundation (q_s) and the non-decaying mineral component of root and rhizome production, so that $q_m = qs + a(R_o T_o + R_h T_h)$. Tidal sediment deposition is added to soil surface (i.e. youngest cohort) only, whereas the mineral component of root and rhizome production enters cohorts at depth. Changes in the mass of organic matter in each cohort, Q_o, follows organic matter production, decomposition, and allochthonous organic matter deposition as described above. Consistent with previous models (e.g. Mudd et al., 2009), organic matter enters the soil profile and contributes to elevation change through belowground biomass turnover. Modeled changes in elevation do not include live biomass because turnover rates are fast relative to the very small changes in live biomass that would occur with an annual model time step. Thus, in each time step, the mass of mineral and organic matter [M L^{-2}] in each cohort is calculated as:

$$Q_m = Q_{m(t-1)} + q_{m(t)} \quad \textbf{(10)}$$

$$Q_o = Q_{o(t-1)} + q_{o(t)}$$

The thickness of each soil cohort, L [L] is then calculated as:

$$L = \frac{Q_m}{\rho_m} + \frac{Q_o}{\rho_o} \quad \textbf{(11)}$$

where ρ_m & ρ_o [M L^{-3}] represent the bulk density of mineral and organic matter, respectively (Morris et al., 2016). The total thickness of the soil column L* [L] is the sum of the thickness of all soil cohorts, L* = $\sum_0^n L$ where n = the number of soil cohorts. The

change in marsh elevation for any timestep (i.e. total accretion rate) [L T^{-1}] is then calculated as:

$$\frac{dz}{dt} = L_t^* - L_{(t-1)}^* \qquad \textbf{(12)}$$

1.5 Organic Matter Content and Carbon Accumulation Rates

The fraction of organic matter in a cohort (o_f) [unitless] (equivalent to LOI- loss on ignition) is calculated by dividing the total mass of organic matter (Q_o) in a cohort by the sum of organic (Q_o) and mineral (Q_m) masses:

$$o_{f=} (Q_o + R_o + R_h)/(Q_o + Q_m + R_o + R_h) \qquad \textbf{(13)}$$

Live roots (R_o) and rhizomes (R_h) are additionally considered in this calculation, so that our organic fraction is consistent with sediment core analyses (i.e. LOI) that typically do not separate live belowground biomass. The fraction of organic matter is converted to the fraction of carbon (c_f) [unitless] following Craft et al., (1991):

$$c_f = 0.4\, o_f + 0.0025\, (o_f)^2 \qquad \textbf{(14)}$$

The total amount of carbon in a given cohort (C_{org}) [M L^{-2}] is given as:

$$C_{org} = c_f Q_o \qquad \textbf{(15)}$$

and the total amount of carbon within the soil column is given as the sum of all carbon in each cohort:

$$C^* = \sum_0^n C_{org} \qquad \textbf{(16)}$$

where n is the number of soil cohorts. Finally, the carbon accumulation rate [M L^{-2} T^{-1}] for a given year represents the total change in the mass of carbon in the soil column, and is calculated as

$$\frac{dC^*}{dt} = C_t^* - C_{(t-1)}^* \qquad \textbf{(17)}$$

2 Model experiments

Model experiments begin with a spin-up period in which the model creates an organic rich soil profile that develops under a constant, slow rate of sea level rise (1 mm yr^{-1}). The model spinup starts with an assigned 1m soil profile composed of 1,000 1 mm thick cohorts with no organic matter. The model then populates the initial mineral stratigraphy with organic matter that evolves dynamically as the balance between organic matter production and decomposition. The model spin up ends when marsh accretion rates equilibrate to the rate of sea level rise and organic matter accumulation rates

become constant. In the first model experiment, we started with the organic rich stratigraphy created during the model spinup and subjected it to a rate of sea level that ensures rapid marsh drowning (25 mm yr^{-1}). The particular rate of rapid sea level rise is arbitrary and was chosen simply to illustrate how modeled processes (vegetation, elevation, and carbon cycling) evolve through time as marshes become more frequently inundated. In the second set of experiments, we explored how different model assumptions lead to changes in marsh resilience. These experiments isolate the effects of novel processes unique to our model, specifically the role of priming and vegetation types that respond differently to eCO_2. As before, these experiments start with the organic rich soil profile created during the model spinup (SLR=1 mm yr^{-1}) and consider the temporal evolution of the marsh under conditions that lead to drowning (SLR=25 mm yr^{-1}). In the final set of model experiments, the model again begins with the organic rich soil profile created during the model spinup period. However, here we subject the soil profile to progressively faster rates of sea level rise (1-12 mm yr^{-1}), with and without the impacts of eCO_2. In these experiments, the model runs until the marsh equilibrates to the new rate of sea level rise, or becomes inundated beyond the limits of vegetation growth (i.e. marsh drowning). Therefore, these final experiments focus on how the interaction between eCO_2, vegetation type, and SLR influences marsh persistence and carbon cycling at equilibrium, rather than the temporal evolution of carbon pools.

Table 1. Key model parameters. * denotes parameters measured at the Smithsonian Global Change Research Wetland or selected to simulate wetlands typical of the site.

Parameter	Description	Value	Source
λ	Tidal amplitude*	0.22 m	Annapolis tide gauge, NOAA 2019
C_t	Suspended sediment concentration*	5 mg L^{-1}	
w_s	Sediment settling velocity	0.0002 m s^{-1}	Marani et al., 2007
α, β, θ	Aboveground biomass coefficients*	C_3 = -4.55E4, 1.50E4, -636 C_4 = -2.63E4, 1.50E4, -1420	Byrd et al., 2017
g	Rhizome:aboveground biomass ratio	ambient = 1 eCO2 = 2	
T_o	Turnover roots*	C_3 species = 1.2 yr^{-1} C_4 species = 1.6 yr^{-1}	Model hindcast
T_h	Turnover rhizomes*	C_3 species = 0.6 yr^{-1} C_4 species = 1.0 yr^{-1}	Model hindcast
γ	Belowground biomass depth distribution*	0.27 m	Megonigal et al., 2020
	Recalcitrant fraction of organic matter	0.16	Mudd et al., 2009
	Labile fraction of organic matter	0.84	Mudd et al., 2009
k_{ref}	Reference decay rate*	Labile = 0.027 yr^{-1} Refractory = 0.0027 yr^{-1}	Model hindcast
v	Priming coefficient*	0.5129	Mueller et al., 2015
ρo	Density of organic matter	0.085 g cm^{-3}	Morris et al., 2016
ρs	Density of mineral matter	1.99 g cm^{-3}	Morris et al., 2016